In: Crystallography: Research, Technology and Applications ISBN: 978-1-62081-574-8
Editors: Misao Hokkaido and Eiko Nagano

Chapter 3

STRUCTURES AND PROPERTIES OF 3D-4F AND 3D CHIRAL SCHIFF BASE COMPLEXES

Tomoaki Hiratsuka, Haruhiko Shibata and Takashiro Akitsu*
Department of Chemistry, Faculty of Science,
Tokyo University of Science, Tokyo, Japan

ABSTRACT

We have prepared several new chiral salen-type Schiff base 3d-4f binuclear (Ln(III)-M(II)) complexes (abbreviated as *LaNi*, *LaCu*, *LaZn*, *NdNi*, *NdCu*, and *NdZn*) and their related 3d mononuclear (M(II)) complexes (abbreviated as *Ni*, *Cu*, and *Zn*). Crystal structures of *Ni*, *LaNi*, *LaCu*, *NdNi* and *LaCu* were determined among them. Temperature dependence of magnetization revealed that Ni(II) ions (as well as Zn(II)) were diamagnetic and Ln(III)-Cu(II) binuclear units indicated ferromagnetic superexchange interactions. We discussed superexchange interactions by means of differences of $\chi_M T$ values and electronic states of Cu(II) ions observed by means of XAS. Moreover, we could observe characteristic chiroptical features in CD bands due to these 3d-4f binuclear units in the solid states.

INTRODUCTION

Structures and magnetic properties of 3d-4f complexes, containing Ln(III) and M(II) or M(III) ions generally, have attracted a great deal of attention in recent years [1]-[10]. However, superexchange interactions are conventionally difficult to understand clearly because of spin-orbit interactions except for Gd(III) ion of $4f^7$ electronic configuration. Therefore, differences of $\Delta\chi_M T$ = $\chi_M T$(Ln[paramagntic] – M[paramagntic]) - $\chi_M T$(Ln[paramagntic] - M'[diamagntic]) between isostructural complexes were sometimes employed to discuss their magnetic interactions [11]. Furthermore, we have also investigated

* Department of Chemistry, Faculty of Science, Tokyo University of Science, 1-3 Kagurazaka, Shinjuku-ku, Tokyo 162-8601, Japan, E-mail address: akitsu@rs.kagu.tus.ac.jp.

to extended to employ this empirical method for cyanide-bridged 3d-4f bimetallic assemblies, $[Ln^{III}(DMA)_2(H_2O)_4M^{III}(CN)_6 \cdot 5H_2O]_n$ bimetallic assemblies (DMA = *N*,*N*-dimethylacetamide, Ln-M = *Nd-Co*, *Gd-Co*, *Sm-Cr*, *Sm-Fe*, *Ho-Fe*, and *Er-Fe*) [12], in other words, $\Delta\chi_M T$ = $\chi_M T$(Ln[paramagntic] – M[diamagnetic]) - $\chi_M T$(Ln'[paramagntic] - M[diamagntic]) as *Nd-Co* and *Gd-Co*, $\Delta\chi_M T$ = $\chi_M T$(Ln[paramagntic] – M[paramagntic]) - $\chi_M T$(Ln[paramagntic] - M'[parmagnetic]) as *Sm-Cr* and *Sm-Fe*, and $\Delta\chi_M T$ = $\chi_M T$(Ln[paramagntic] – M[paramagntic]) - $\chi_M T$(Ln'[paramagntic] - M[paramagnetic]) as *Ho-Fe* and *Er-Fe*. The extended examination suggested that diamagnetic transition metal ion M' was one of the important conditions for limitation in this approach of cyanide-bridged 3d-4f bimetallic assemblies. It may be necessary to use some other physical measurements for this purpose.

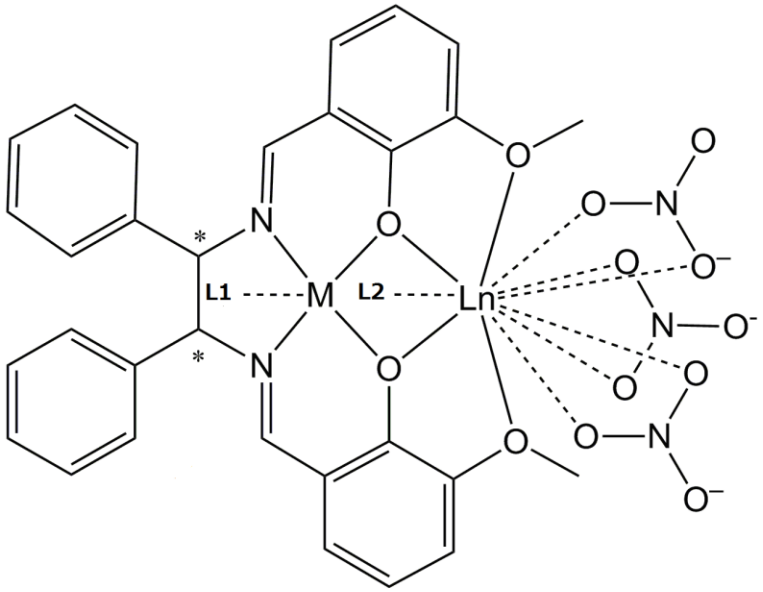

Ni:Ln=none, M=Ni, L1=none, L2=none

Cu:Ln=none, M=Cu, L1=none, L2=none

Zn:Ln=none, M=Zn, L1=none, L2=none

LaNi:Ln=La, M=Ni, L1=none, L2=MeOH

LaCu:Ln=La, M=Cu, L1=none, L2=MeOH

LaZn:Ln=La, M=Zn, L1=MeOH, L2=none

NdNi:Ln=none, M=Ni, L1=none, L2=MeOH

NdCu:Ln=none, M=Cu, L1=MeOH, L2=none

NdZn:Ln=none, M=Zn, L1=MeOH, L2=none

Figure 1. Molecular structures of complexes. Crystalline solvents were omitted for clarity.

In this context, not only d-d [13,14] but also d-f [15,16] heterodinuclear Schiff base complexes may exhibit characteristic chiroptical properties, which are different from that of mononuclear complexes containing sole d -or f-ions. Herein, we have prepared several new chiral salen-type Schiff base 3d-4f binuclear (Ln(III)-M(II)) complexes (abbreviated as *LaNi*, *NdNi*, *LaCu*, and *NdCu)* and the related 3d mononuclear (M(II)) complexes (abbreviated as *Ni*, *Cu*, and *Zn*) (Figure 1). As revealed later, La(III), Ni(II), and Zn(II) ions are diamagnetic, while Nd(III) and Cu(II) ions are paramagnetic. Therefore, *NdCu* is the only candidate to show ferromagnetism due to superexchange interactions, which can be estimated based on the difference of $\chi_M T$ values. Interestingly, we have successfully observed characteristic chiroptical bands in CT region due to 3d-4f binuclear in solid state CD spectra, which is derived from systematic comparison with M(II)[diamagnetic], M(II)[paramagnetic], Ln(III)[diamagnetic]-M(II)[diamagnetic], Ln(III)[paramagnetic]-M(II)[diamagnetic], Ln(III)[diamagnetic]-M(II)[paramagnetic], and Ln(III)[paramagnetic]-M(II)[paramagnetic]. To our knowledge, it is the first attempt to discuss correlation between structures and solid-state chiroptical properties in exchange-coupled binuclear 3d-4f systems and mononuclear 3d complexes.

EXPERIMENTAL SECTION

Materials

All reagents and solvents (Wako, TCI, and Aldrich) were commercially available and were used as purchased without further purification.

Preparations

Preparation of Ni. To a solution of *o*-vanillin (0.3055 g, 2.00 mmol) dissolved in methanol (50 mL), (*1R,2R*)-(+)-1,2-diphenyl-ethylenediamine (0.2133 g, 1.00 mmol) was added dropwise and stirred at 313 K for 2 h to give yellow solution of ligand. Nickel(II) acetate tetrahydrate (0.2213 g, 1.00 mmol) was added to the resulting solution give red solution of the complex. After stirring for 2 h, this crude red compound was filtered and recrystallized from methanol/diethyl ether to give orange prismatic single crystals suitable for X-ray analysis containing solvents. Yield 0.4717 g (80.20 %). IR (KBr) 1621 cm^{-1} (C = N).

Preparation of Cu. To a solution of *o*-vanillin (0.3049 g, 2.00 mmol) dissolved in methanol (50 mL), (*1R,2R*)-(+)-1,2-diphenyl-ethylenediamine (0.2130 g, 1.00 mmol) was added dropwise and stirred at 313 K for 2 h to give yellow solution of ligand. Copper(II) acetate monohydrate (0.2027 g, 1.00 mmol) was added to the resulting solution give green solution of the complex. After stirring for 2 h, this crude green compound was filtered and recrystallized from methanol/diethyl ether. Yield 0.4006 g (80.89 %). IR (KBr) 1626 cm^{-1} (C = N).

Preparation of Zn. To a solution of *o*-vanillin (0.3049 g, 2.00 mmol) dissolved in methanol (50 mL), (*1R,2R*)-(+)-1,2-diphenyl-ethylenediamine (0.2128 g, 1.00 mmol) was added dropwise and stirred at 313 K for 2 h to give yellow solution of ligand. Zinc(II) acetate

dihydrate (0.2199 g, 1.00 mmol) was added to the resulting solution give yellow solution of the complex. After stirring for 2 h, this crude white compound was filtered and recrystallized from methanol/diethyl ether. Yield 0.4020 g (80.89 %). IR (KBr) 1626 cm^{-1} (C = N).

Preparation of LaNi. To a solution of *o*-vanillin (0.3050 g, 2.00 mmol) dissolved in methanol (50 mL), (*1R,2R*)-(+)-1,2-diphenyl-ethylenediamine (0.2139 g, 1.00 mmol) was added dropwise and stirred at 313 K for 2 h to give yellow solution of ligand. Nickel(II) acetate tetrahydrate (0.2219 g, 1.00 mmol) was added to give rise to red solution of the complex. After stirring for 2 h, lanthanum(III) nitrate hexahydrate (0.4342 g, 1.00 mmol) was added and refluxed at 373 K for 4h to yield red solution with orange precipitates. This crude red compound was filtered and recrystallized from methanol/diethyl ether to give orange prismatic single crystals suitable for X-ray analysis containing solvents. Yield 0.6608 g (73.90 %). IR (KBr) 1624 cm^{-1} (C = N).

Preparation of LaCu. To a solution of *o*-vanillin (0.3054 g, 2.00 mmol) dissolved in methanol (50 mL), (*1R,2R*)-(+)-1,2-diphenyl-ethylenediamine (0.2139 g, 1.00 mmol) was added dropwise and stirred at 313 K for 2 h to give yellow solution of ligand. Copper(II) acetate monohydrate (0.2195 g, 1.00 mmol) was added to give rise to green solution of the complex. After stirring for 2 h, lanthanum(III) nitrate hexahydrate (0.4345 g, 1.00 mmol) was added and refluxed at 373 K for 4h to yield dark green solution with purple precipitates. This crude purple compound was filtered and recrystallized from methanol/diethyl ether to give purple prismatic single crystals suitable for X-ray analysis containing solvents. Yield 0.6617 g (73.60 %). IR (KBr) 1626 cm^{-1} (C = N).

Preparation of LaZn. To a solution of *o*-vanillin (0.3048 g, 2.00 mmol) dissolved in methanol (50 mL), (*1R,2R*)-(+)-1,2-diphenyl-ethylenediamine (0.2141 g, 1.00 mmol) was added dropwise and stirred at 313 K for 2 h to give yellow solution of ligand. Zinc(II) acetate dihydrate (0.2199 g, 1.00 mmol) was added to give rise to yellow solution of the complex. After stirring for 2 h, lanthanum(III) nitrate hexahydrate (0.4360 g, 1.00 mmol) was added and refluxed at 373 K for 4h to yield yellow solution with white precipitates. This crude white compound was filtered and recrystallized from methanol/diethyl ether. Yield 0.4174 g (46.33 %). IR (KBr) 1629 cm^{-1} (C = N).

Preparation of NdNi. To a solution of *o*-vanillin (0.3044 g, 2.00 mmol) dissolved in methanol (50 mL), (*1R,2R*)-(+)-1,2-diphenyl-ethylenediamine (0.2129 g, 1.00 mmol) was added dropwise and stirred at 313 K for 2 h to give yellow solution of ligand. Nickel(II) acetate tetrahydrate (0.2213 g, 1.00 mmol) was added to give rise to red solution of the complex. After stirring for 2 h, neodymium(III) nitrate hexahydrate (0.4378 g, 1.00 mmol) was added and refluxed at 373 K for 4h to yield red solution with orange precipitates. This crude orange compound was filtered and recrystallized from methanol/diethyl ether to give orange prismatic single crystals suitable for X-ray analysis containing solvents. Yield 0.5928 g (65.9 %). IR (KBr) 1621 cm^{-1} (C = N).

Preparation of NdCu. To a solution of *o*-vanillin (0.3056 g, 2.00 mmol) dissolved in methanol (50 mL), (*1R,2R*)-(+)-1,2-diphenyl-ethylenediamine (0.2124 g, 1.00 mmol) was added dropwise and stirred at 313 K for 2 h to give yellow solution of ligand. Copper(II) acetate monohydrate (0.1990 g, 1.00 mmol) was added to give rise to green solution of the complex. After stirring for 2 h, neodymium (III) nitrate hexahydrate (0.4415 g, 1.00 mmol) was added and refluxed at 373 K for 4h to yield dark green solution with purple precipitates. This crude purple compound was filtered and recrystallized from methanol/diethyl ether to

give orange prismatic single crystals suitable for X-ray analysis containing solvents. Yield 0.6204 g (66.6 %). IR (KBr) 1630 cm^{-1} (C = N).

Preparation of NdZn. To a solution of *o*-vanillin (0.3044 g, 2.00 mmol) dissolved in methanol (50 mL), (*1R,2R*)-(+)-1,2-diphenyl-ethylenediamine (0.2140 g, 1.00 mmol) was added dropwise and stirred at 313 K for 2 h to give yellow solution of ligand. Zinc(II) acetate dihydrate (0.2219 g, 1.00 mmol) was added to give rise to yellow solution of the complex. After stirring for 2 h, neodymium (III) nitrate hexahydrate (0.4380 g, 1.00 mmol) was added and refluxed at 373 K for 4h to yield yellow solution with white precipitates. This crude white compound was filtered and recrystallized from methanol/diethyl ether. Yield 0.4034 g (44.51 %). IR (KBr) 1626 cm^{-1} (C = N).

Physical Measurements

Elemental analyses (C, H, N) were carried out with a Perkin-Elmer 2400II CHNS/O analyzer at Tokyo University of Science. Infrared spectra were recorded as KBr pellets on a JASCO FT-IR 4200 plus spectrophotometer equipped with polarizer in the range of 4000-400 cm^{-1} at 298 K. Diffuse reflectance electronic spectra were measured on a JASCO V-570 UV/VIS/NIR spectrophotometer equipped with an integrating sphere in the range of 800-200 nm at 298 K. Circular dichroism (CD) spectra were measured as KBr pellets on a JASCO J-820 spectropolarimeter in the range of 800-300 nm at 298 K. Powder XRD patterns were also measured by using synchrotron radiation beamline at KEK-PF BL-8B with 8 keV (λ = 1.54184 Å) with a RIGAKU imaging plate. The $Cu2p_{3/2}$ and $Cu2p_{1/2}$ peaks of XAS (soft X-ray absorption spectra) were measured at KEK PF BL-19B under variable temperature. The spectra were corrected by the standard Au sample. The magnetic properties were investigated with a Quantum Design MPMS-XL superconducting quantum interference device magnetometer (SQUID) at an applied field 1000 Oe in a temperature range 2-300 K. Powder samples were measured in a pharmaceutical cellulose capsule. The apparatus signals and the diamagnetic corrections were evaluated from the analogous diamagnetic *LaZn* complex.

X-Ray Crystallography

Red prismatic (*Ni*), red prismatic (*LaNi*), purple prismatic (*LaCu*), red prismatic (*NdNi*), and purple prismatic (*NdCu*), single crystals were glued on top of a glass fiber and coated with a thin layer of epoxy resin to measure the diffraction data. Intensity data were collected on a Bruker APEX2 CCD diffractometer with graphite monochromated Mo Kα radiation (λ = 0.71073 Å). Data analysis was carried out with a SAINT program package. The structures were solved by direct methods with a SHELXS-97 [17] and expanded by Fourier techniques and refined by full-matrix least-squares methods based on F^2 using the program SHELXL-97 [17]. An empirical absorption correction was applied by a program SADABS. All non-hydrogen atoms were readily located and refined by anisotropic thermal parameters. All hydrogen atoms except for some atoms of O-H terminal groups were located at geometrically calculated positions and refined using riding models. Unfortunately, suitable single crystals of the rest complexes could not be obtained.

Crystallographic data for Ni. $C_{31}H_{30}NiN_2O_5$,crystal size 0.27 mm × 0.26 mm × 0.22 mm, M_w = 587.289, triclinic, space group *P1* (#1), *a* = 10.3034(18)Å, *b* = 10.908(2) Å, *c* = 13.131(2) Å, α = 84.922(2)°, β = 72.655(2)°, γ = 76.395(2)°, *V* = 1368.9(4) Å^3, *Z* = 2, D_{calc} = 1.425 mg/m^3, F(000) = 616.0, R_1 = 0.0491, wR_2 = 0.1501 (7055 reflections), *S* = 0.967, Flack parameter = 363(18). (where $R_1 = \Sigma||F_o|-|F_c||/\Sigma|F_o|$. $R_w = (\Sigma w(|F_o|-|F_c|)^2 /\Sigma w|F_o|^2)^{1/2}$, $w = 1/(\sigma^2(F_o) + (0.1P)^2)$, $P = (F_{o2} + 2F_{c2})/3$).

Crystallographic data for LaNi. $C_{31}H_{30}LaNiN_5O_{14}$, crystal size 0.30 mm × 0.27 mm × 0.25 mm, M_w = 894.194, monoclinic, space group $P2_1$ (#4), *a* = 10.5909(9) Å, *b* = 20.9511(18) Å, *c* = 15.9571(14) Å, β = 101.7460(10)°, *V* = 3466.6(5) Å^3, *Z* = 4, D_{calc} = 1.713 g/cm^3, F(000) = 1792.0, R_1 = 0.0403, wR_2 = 0.1282 (14616 reflections), *S* = 0.834, Flack parameter = 0.006(15). (where $R_1 = \Sigma||F_o|-|F_c||/\Sigma|F_o|$. $R_w = (\Sigma w(|F_o|-|F_c|)^2 /\Sigma w|F_o|^2)^{1/2}$, $w = 1/(\sigma^2(F_o) + (0.1P)^2)$, $P = (F_{o2} + 2F_{c2})/3$).

Crystallographic data for LaCu. $C_{31}H_{30}LaCuN_5O_{14}$, crystal size 0.15 mm × 0.14 mm × 0.10 mm, M_w = 899.046, monoclinic, space group $P2_1$ (#4), *a* = 10.5839(5) Å, *b* = 20.9651(9) Å, *c* = 15.7310(7) Å, β = 101.7080(10)°, *V* = 3418.0(3) Å^3, *Z* = 4, D_{calc} = 1.747 g/cm^3, F(000) = 1796.0, R_1 = 0.0403, wR_2 = 0.1055 (13291 reflections), *S* = 0.837, Flack parameter = -0.005(10). (where $R_1 = \Sigma||F_o|-|F_c||/\Sigma|F_o|$. $R_w = (\Sigma w(|F_o|-|F_c|)^2 /\Sigma w|F_o|^2)^{1/2}$, $w = 1/(\sigma^2(F_o) + (0.1P)^2)$, $P = (F_{o2} + 2F_{c2})/3$).

Crystallographic data for NdNi. $C_{31}H_{30}NdCuN_5O_{14}$, crystal size 0.37 mm × 0.25 mm × 0.25 mm, M_w = 899.528, monoclinic, space group $P2_1$ (#4), *a* = 10.5443(13) Å, *b* = 20.829(3) Å, *c* = 15.7921(19) Å, β = 101.730(2)°, *V* = 3396.0(7) Å^3, *Z* = 4, D_{calc} = 1.759 g/cm^3, F(000) = 1804.0, R_1 = 0.0459, wR_2 = 0.1437 (14230 reflections), *S* = 0.874, Flack parameter = -0.006(17). (where $R_1 = \Sigma||F_o|-|F_c||/\Sigma|F_o|$. $R_w = (\Sigma w(|F_o|-|F_c|)^2 /\Sigma w|F_o|^2)^{1/2}$, $w = 1/(\sigma^2(F_o) + (0.1P)^2)$, $P = (F_{o2} + 2F_{c2})/3$).

Crystallographic data for NdiCu. $C_{32}H_{33}NdcuN_5O_{15}$, crystal size 0.24 mm × 0.10 mm × 0.07 mm, M_w = 931.570, monoclinic, space group *C2* (#5), *a* = 9.3229(15) Å, *b* = 15.884(3) Å, *c* = 23.920(4) Å, β = 95.049(2)°, *V* = 3528.4(10) Å^3, *Z* = 4, D_{calc} = 1.763g/cm^3, F(000) = 1888.0, R_1 = 0.0337, wR_2 = 0.0984 (14429 reflections), *S* = 0.708, Flack parameter = 0.018(10). (where $R_1 = \Sigma||F_o|-|F_c||/\Sigma|F_o|$. $R_w = (\Sigma w(|F_o|-|F_c|)^2 /\Sigma w|F_o|^2)^{1/2}$, $w = 1/(\sigma^2(F_o) + (0.1P)^2)$, $P = (F_{o2} + 2F_{c2})/3$).

RESULTS AND DISCUSSION

Crystal Structures

Stepwise reaction of chiral Schiff base ligands, 3d (Ni(II), Cu(II), and Zn(II)) ions, and 4f (La(III) and Nd(III)) ions systematically yielded 3d mononuclear or 3d-4f heteronuclear complexes as microcrystalline precipitates. Single crystals were grown from methanol/diethyl ether solvents (and metal source reagents contain crystalline water) by vapor diffusion. Differences of compositions are found in methanol molecules (present or absent and as axial ligand or crystalline solvent). Overall paired structures as an asymmetric unit are connected by intermolecular hydrogen bonds of methanol molecules and nitrate ions acting as ligands at least for five complexes, because for the five structures determined contain La(III) and Nd(III) ions having similar size if any. Moreover, bond distances and angles of organic

moieties are common values as Schiff base ligands [15, 16], in particular relatively short C=N double bond distances of imine groups. Phenyl groups connected to asymmetric carbon atoms of (*R,R*)-configuration exist on opposite sides of the molecular plane. The magnitude of dihedral angles of C(phenyl)-C(asymmetric carbon)-C(asymmetric carbon)-C-(phenyl), namely C10-C9-C24-C25 and C40-C39-C54-C55, takes within the range from 59 to 69°, which means that phenyl groups on the asymmetric carbon atoms are located to equatorial direction regardless of differences of crystal packing. As for structurally characterized *Ni*, *LaNi*, *LaCu*, *NdNi* and *NdCu* complexes (Figures 2, 3, 4, 5, and 6, respectively), Ni(II) and Cu(II) ions afford a four-coordinated square planar coordination environment. According to *trans*-N-M-O bond angles (deviation from ideal value of 180°), *Ni* keeps planarity of coordination environment, and degree of distortion of *LaCu* and *NdCu* are larger than that of *LaNi* and *NdNi*. It should be noted that *NdCu* has semi-coordinated methanol molecules on the axial sites, which ascribes to significant distortion of a square-planar coordination environment with *trans*-N-M-O bond angles less than 170°.

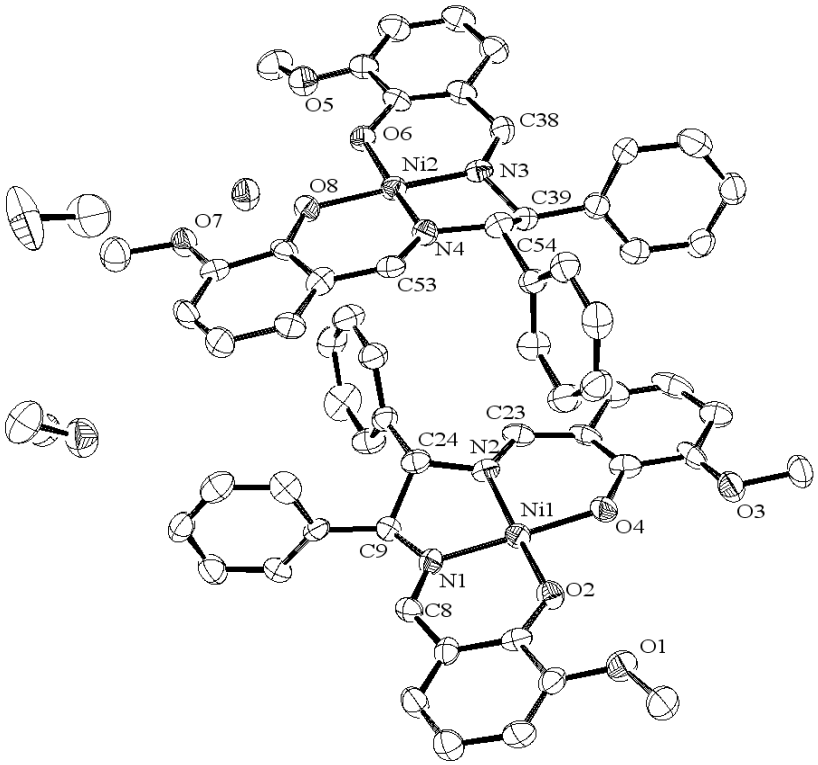

Figure 2. An ORTEP drawing of *Ni* showing the atom-labeling scheme Displacement ellipsoids are drawn at the 50 % probability level. Hydrogen atoms are omitted for clarity. Selected bond distances (Å) and angles (˚): Ni1-O2 = 1.827(6), Ni1-N1 = 1.851(6), Ni1-O4 = 1.861(6), Ni1-N2 = 1.851(6), Ni2-O6 = 1.864(5), Ni2-N3 = 1.840(7), Ni2-O8 = 1.848(5), Ni2-N4 = 1.844(7), O2-Ni1-N1 = 95.1(18), N1-Ni1-N2 = 85.5(3), N2-Ni- O4 = 178.2(3), N2-Ni1-O2 = 86.3(2), O2-Ni1-N2 = 172.6(3), O4-Ni1-N1 = 178.2(3), O6-Ni2-N3 = 93.8(3), N3-Ni2-N4 = 86.3(3), N4-Ni2-O8 = 94.9(3), O8-Ni2-O6 = 85.3(2), O6-Ni2-N4 = 174.53(3), O8-Ni2-N3 = 176.7(3).

In contrast to general tendency that Cu(II) and Zn(II) complexes are easy to coordinate axial methanol ligands, whereas Ni(II) ones are hard to, structures of the analogous Zn(II) complexes are almost similar to that of Ni(II) ones based on XRD patterns. On the other hand, La(III) and Nd(III) ions afford a ten-coordinated prism [LnO_{10}] coordination environment regardless of lanthanide contraction. However, as far as crystal structures are determined, *Ni* contains crystalline water as well as methanol solvent, *LaNi*, *NdNi*, and *LaCu* contain methanol molecules coordinated to La(III) or Nd(III) ions, and *NdCu* has methanol semi-coordinated to Cu(II) ion as described above.

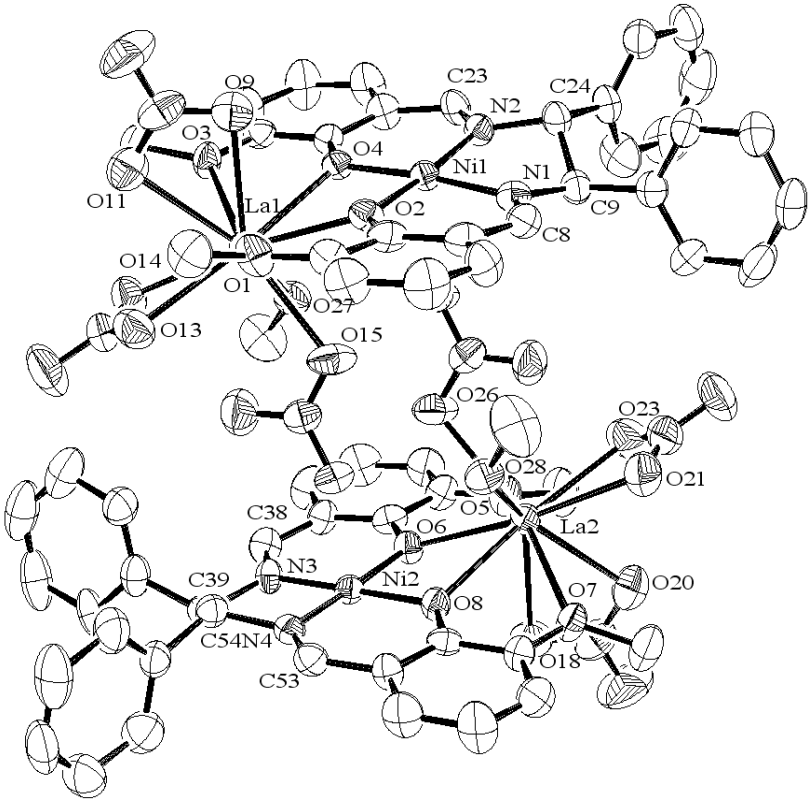

Figure 3. An ORTEP drawing of *LaNi* showing the atom-labeling scheme Displacement ellipsoids are drawn at the 50 % probability level. Hydrogen atoms are omitted for clarity. Selected bond distances (Å) and angles (˚): Ni1-O2 = 1.838(5), Ni1-N1 = 1.831(6), Ni1-O4 = 1.848(5), Ni1-N2 = 1.847(5), Ni2-O6 = 1.861(4), Ni2-N3 = 1.842(6), Ni2-O8 = 1.862(5), Ni2-N4 = 1.866(6), La1-O1 = 2.680(6), La1-O2 = 2.511(5), La1-O3 = 2.678(4), La1-O4 = 2.542(5), La1-O9 = 2.629(7), sLa1-O11 = 2.614(6), La1-O13 = 2.606(7), La1-O14 = 2.583(6), La1-O15 = 2.612(5), La1-O27 = 2.578(5), La2-O5 = 2.654(6), La2-O6 = 2.523(5), La2-O7 = 2.711(5), La2-O8 = 2.526(5), La2-O18 = 2.645(6), La2-O20 = 2.594(6), La2-O21 = 2.580(7), La2-O23 = 2.655(8), La2-O26 = 2.680(6), La2-O28 = 2.593(5), O2-Ni1-N1 = 95.2(2), N1-Ni1-N2 = 86.6(3), N2-Ni1-O4 = 95.5(2), O4-Ni1-O2 = 83.1(2), O2-Ni1-N2 = 175.1(2), O4-Ni1-N1 = 174.2(2), O6-Ni2-N3 = 94.9(2), N3-Ni2-N4 = 87.2(3), N4-Ni2-O8 = 95.3(2), O8-Ni2-O6 = 82.7(2), O6-Ni2-N4 = 176.4(3), O8-Ni2-N3 = 177.0 (2).

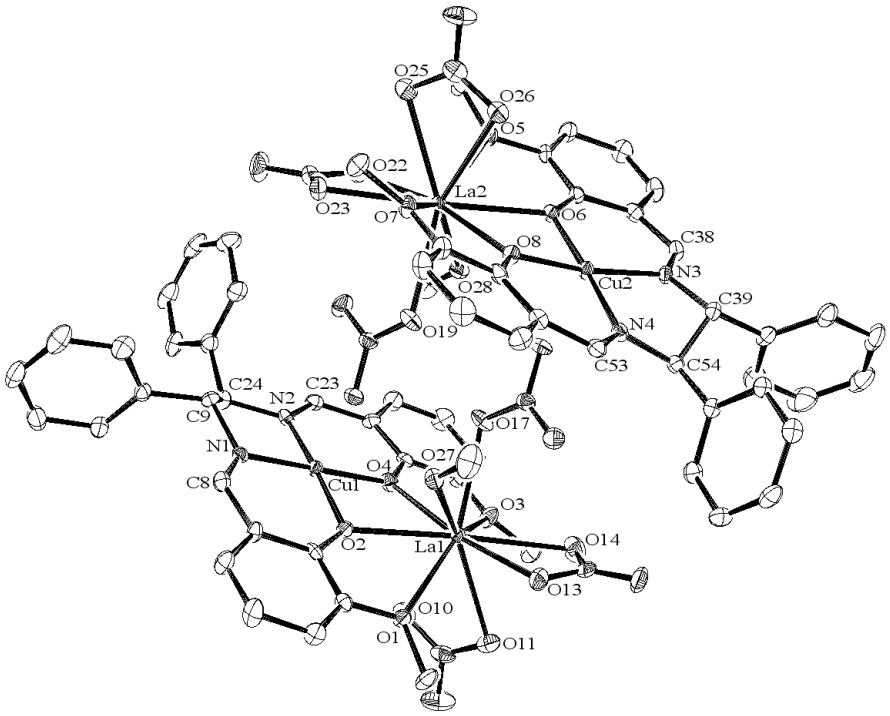

Figure 4. An ORTEP drawing of *LaCu* showing the atom-labeling scheme Displacement ellipsoids are drawn at the 50 % probability level. Hydrogen atoms are omitted for clarity. Selected bond distances (Å) and angles (˚): Cu1-O2 = 1.903(4), Cu1-N1 = 1.921(4), Cu1-O4 = 1.904(3), Cu1-N2 = 1.912(5), Cu2-O6 = 1.900(4), Cu2-N3 = 1.931(4), Cu2-O8 = 1.904(3), Cu2-N4 = 1.912(4), La1-O1 = 2.726(3), La1-O2 = 2.515(3), La1-O3 = 2.682(4), La1-O4 = 2.497(4), La1-O10 = 2.627(4), La1-O11 = 2.592(4), La1-O13 = 2.591(4), La1-O14 = 2.622(5), La1-O17 = 2.641(3), La1-O27 = 2.571(4), La2-O5 = 2.715(3), La2-O6 = 2.518(3), La2-O7 = 2.710(4), La2-O8 = 2.4951(4), La2-O19 = 2.622(3), La2-O22 = 2.594(4), La2-O23 = 2.626(4), La2-O25 = 2.583(4), La2-O26 = 2.615(4), La2-O28 = 2.570(4), O2-Cu1-N1 = 95.20(16), N1-Cu1-N2 = 86.88(18), N2-Cu1-O4 = 94.87(17), O4-Cu1-O2 = 83.21(15), O2-Cu1-N2 = 173.26(16), O4-Cu1-N1 = 177.80(18), O6-Cu2-N3 = 95.43(16), N3-Cu2-N4 = 86.42(17), N4-Cu2-O8 = 94.38(16), O8-Cu2-O6 = 84.05(15), O6-Cu2-N4 = 177.55(16), O8-Cu2-N3 = 170.85 (16).

In order to confirm approximately isostructural features among the rest of complexes, powder XRD patterns were measured with λ =1.54184 Å and their predominant diffraction peaks (2θ/degree) were observed as follows:

LaNi: 7.018, 8.932, 9.831, 10.469, 11.832, 13.311, 14.123, 14.500, 15.544, 17.342, 17.922, 18.705, 20.097, 21.750, 22.388, 23.403, 23.838, 35.148.

LaCu: 7.192, 8.439, 9.338, 9.541, 10.266, 11.281, 11.687, 12.035, 12.615, 14.123, 14.442, 16.385, 16.965, 17.487, 19.662, 20.619, 21.460, 22.736, 23.287, 24.679, 25.520, 27.347, 28.014, 33.988.

LaZn: 6.989, 7.482, 10.875, 11.600, 12.354, 12.644, 12.905, 14.036, 14.384, 16.269, 18.270, 21.547, 22.852, 23.519, 26.825, 28.507, 31.146, 32.828, 34.713.

NdNi: 7.366, 8.062, 8.787, 9.425, 10.411, 11.426, 12.093, 13.398, 14.181, 14.964, 15.225, 16.385, 16.733, 18.415, 18.937, 21.199, 22.939, 24.099, 26.970, 30.131, 30.508.

NdCu: 6.525, 7.888, 9.947, 10.382, 11.194, 12.267, 13.079, 14.384, 15.892, 18.531, 20.648, 21.460, 24.157, 24.563, 25.578, 26.506, 27.579, 36.453.

NdZn: 7.482, 8.091, 8.874, 9.483, 10.527, 11.600, 14.384, 16.269, 18.27, 18.955, 21.199, 24.128, 26.999, 30.537.

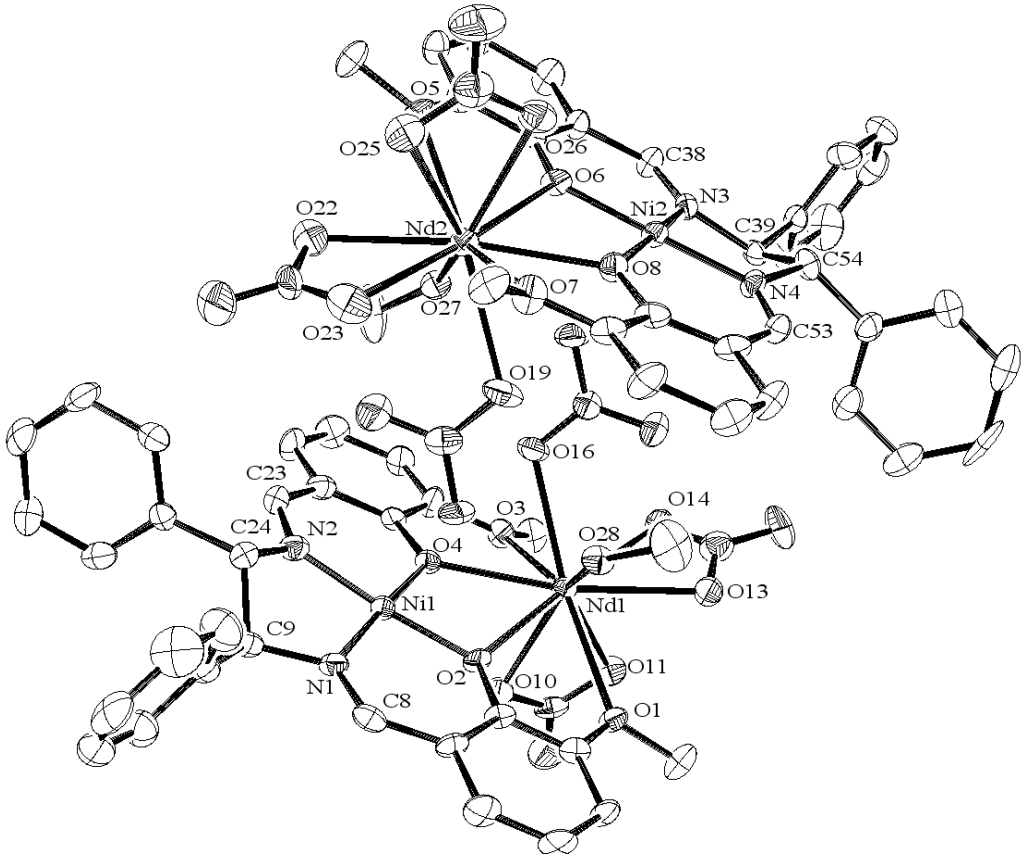

Figure 5. An ORTEP drawing of *NdNi* showing the atom-labeling scheme Displacement ellipsoids are drawn at the 50 % probability level. Hydrogen atoms are omitted for clarity. Selected bond distances (Å) and angles (˚): Ni1-O2 = 1.842(6), Ni1-N1 = 1.842(7), Ni1-O4 = 1.841(6), Ni1-N2 = 1.829(8), Ni2-O6 = 1.864(7), Ni2-N3 = 1.855(7), Ni2-O8 = 1.867(6), Ni2-N4 = 1.842(7), Nd1-O1 = 2.638(5), Nd1-O2 = 2.476(6), Nd1-O3 = 2.634(8), Nd1-O4 = 2.444(6), Nd1-O10 = 2.564(7), Nd1-O11 = 2.526(6), Nd1-O13 = 2.527(7), Nd1-O14 = 2.562(7), Nd1-O16 = 2.532(5), Nd1-O28 = 2.505(6), Nd2-O5 = 2.645(5), Nd2-O6 = 2.473(6), Nd2-O7 = 2.635(7), Nd2-O8 = 2.458(6), Nd2-O19 = 2.549(6), Nd2-O22 = 2.516(8), Nd2-O23 = 2.561(9), Nd2-O25 = 2.553(7), Nd2-O26 = 2 2.517(7), Nd2-O27 = 2.571(7),O2-Ni1-N1 = 96.5(3), N1-Ni1-N2 = 86.3(3), N2-Ni1-O4 = 95.1(3), O4-Ni1-O2 = 60.58(19), O2-Ni1-N2 = 175.1(3), O4-Ni1-N1 = 175.0(3), O6-Ni2-N3 = 95.4(3), N3-Ni2-N4 = 87.6(3), N4-Ni2-O8 = 95.0(3), O8-Ni2-O6 = 82.1(3), O6-Ni2-N4 = 176.2(3), O8-Ni2-N3 = 175.7(3).

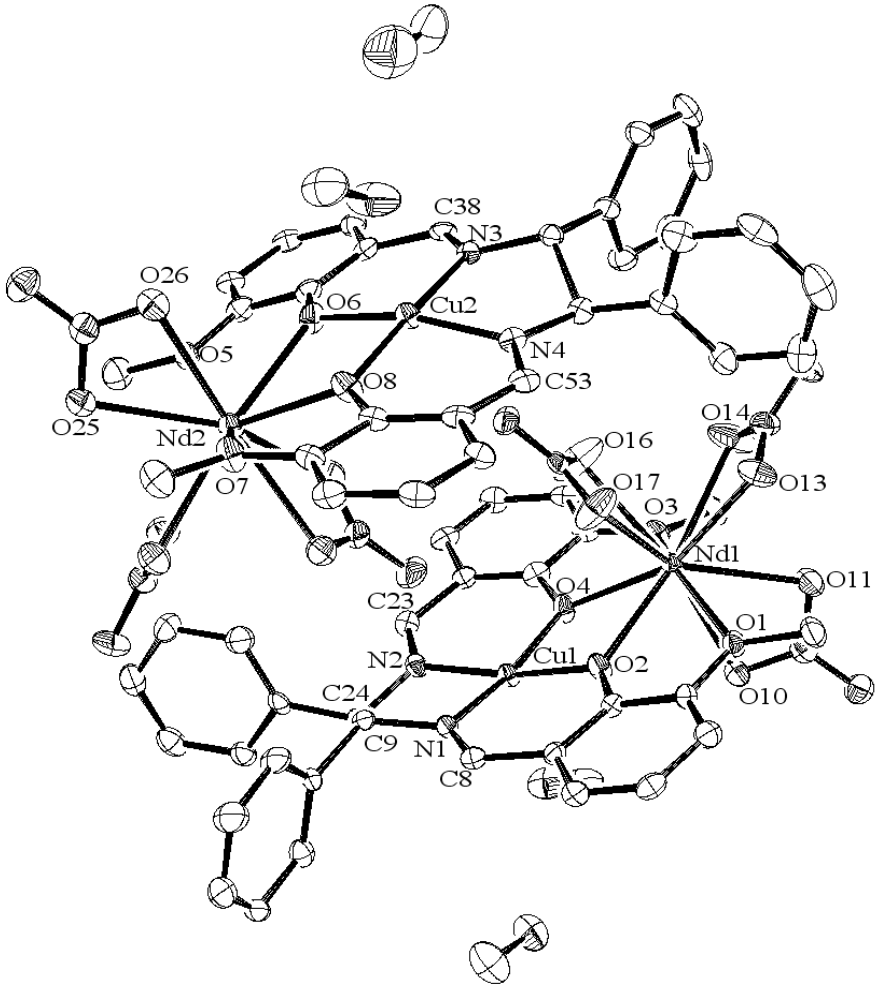

Figure 6. An ORTEP drawing of *NdCu* showing the atom-labeling scheme Displacement ellipsoids are drawn at the 50 % probability level. Hydrogen atoms are omitted for clarity. Selected bond distances (Å) and angles (˚): Cu1-O2 = 1.924(3), Cu1-N1 = 1.921(5), Cu1-O4 = 1.916(4), Cu1-N2 = 1.945(4), Cu2-O6 = 1.922(4), Cu2-N3 = 1.924(4), Cu2-O8 = 1.916(4), Cu2-N4 = 1.940(4), Nd1-O1 = 2.638(4), Nd1-O2 = 2.404(3), Nd1-O3 = 2.625(4), Nd1-O4 = 2.418(3), Nd1-O10 = 2.547(4), Nd1-O11 = 2.509(4), Nd1-O13 = 2.564(4), Nd1-O14 = 2.580(5), Nd1-O16 = 2.508(5), Nd1-O17 = 2.529(4), Nd2-O5 = 2.628(4), Nd2-O6 = 2.440(4), Nd2-O7 = 2.654(4), Nd2-O8 = 2.384(3), Nd2-O19 = 2.506(4), Nd2-O20 = 2.552(4), Nd2-O22 = 2.556(4), Nd2-O23 = 2.600(4), Nd2-O25 = 2.497(4), Nd2-O26 = 2.553(4), O2-Cu1-N1 = 95.05(18), N1-Cu1-N2 = 86.02(19), N2-Cu1-O4 = 94.69(16), O4-Ni1-O2 = 85.35(15), O2-Cu1-N2 = 170.21(18), O4-Cu1-N2 = 168.54(19), O6-Ni2-N3 = 96.17(18), N3-Cu2-N4 = 86.20(18), N4-Cu2-O8 = 93.92(17), O8-Cu2-O6 = 82.69(15), O6-Cu2-N4 = 165.81(17), O8-Cu2-N3 = 175.73(19).

Magnetic Properties

The magnetic behavior for the 3d-4f complexes has been investigated at 2-300 K as polycrystalline samples under 1000 Oe. Figure 7 shows temperature dependence of the

product of the molar magnetic susceptibilities ($\chi_M T$) and temperature (T) for mononuclear complexes (*Ni*, *Cu*, and *Zn*), La(III) [diamagnetic]-M(II) binuclear complexes (*LaNi*, *LaCu*, and *LaZn*), and Nd(III) [paramagnetic]-M(II) binuclear complexes (*NdNi*, *NdCu*, and *NdZn*). Comparison with diamagnetic *Zn*, *Ni* of a four-coordinated square planar coordination environment also exhibits diamagnetic behavior. After applying diamagnetic correction with *Zn*, the $\chi_M T$ value (*Cu*-*Zn*) of 0.296 emu mol^{-1}K (μ = 1.73 B.M.; spin-only theoretical value is μ = 1.73 B.M.) for *Cu* at 300 K is in agreement with paramagnetic contribution of Cu(II) of s = 1/2. By the way, *LaNi* and *LaZn* must be diamagnetic, while only *LaCu* can be paramagnetic because of Cu(II) ion. Indeed, the $\chi_M T$ value (*LaCu*-*LaZn*) of 0.522 emu mol^{-1}K (μ = 2.04 B.M.; spin-only theoretical value is μ = 1.54 B.M.) at 300 K also indicates paramagnetic behabior of *LaCu*. Finally, *NdNi* and *NdZn* are diamagnetic according to magnetic data. According to the $\chi_M T$ value (*Cu*-*Zn*) of 0.731 emu mol^{-1}K at 300 K (μ = 2.41 B.M.; spin-only theoretical value is μ = 4.89 B.M.), only paramagnetic *NdCu* can exhibit superexchange interaction and significant contribution of orbital angular moment to explain large deviation. In the low temperature region, slight decrease of the $\chi_M T$ values suggests antiferromagnetic interactions in the 3d-4f units for *NdCu*.

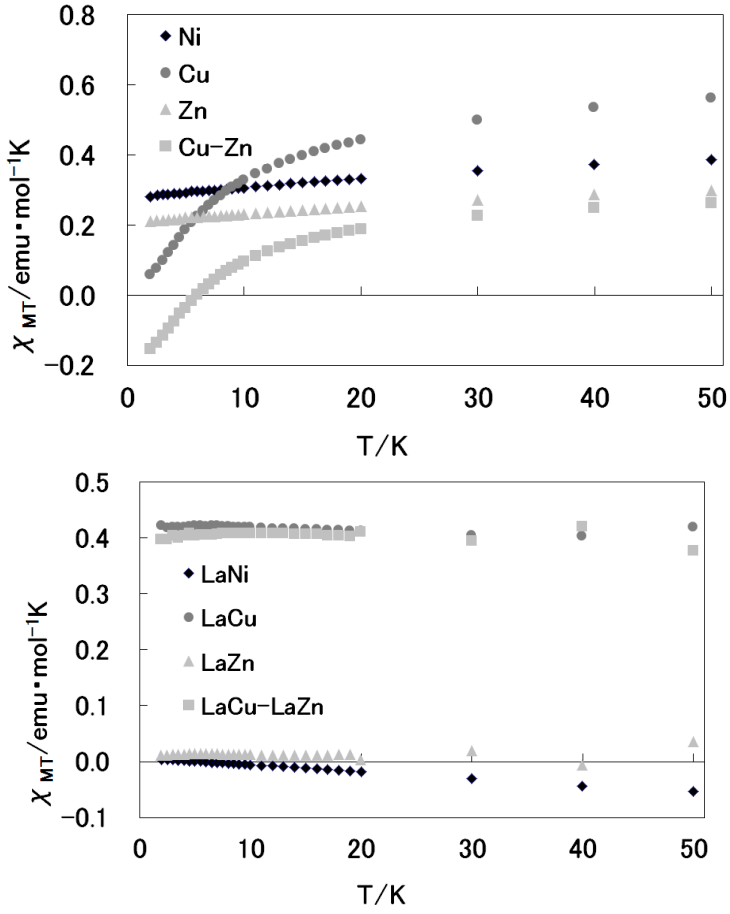

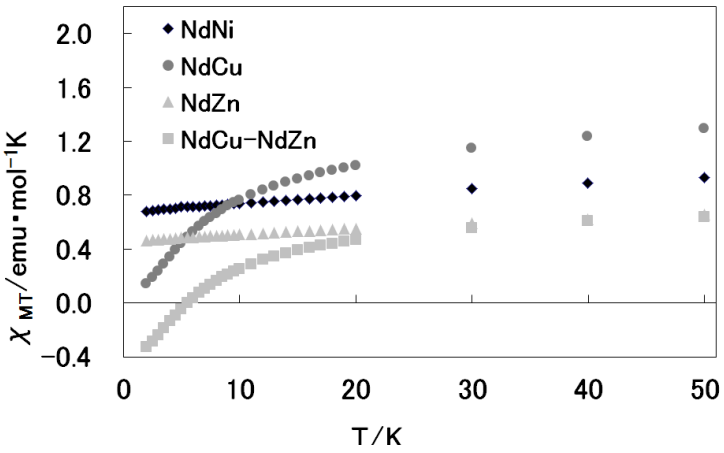

Figure 7. The $\chi_M T$ (and their differences) vs T plots for mononuclear, La(III), and Nd(III) complexes at 0.1 T.

XAS Spectra

In order to discuss the influence of 4f ions on Cu(II) ions in (potentially ferromagnetic) *Cu*, *LaCu*, and *NdCu*, we measured XAS for electronic states of inner shell. The XAS spectra for *Cu*, *LaCu*, and *NdCu* are shown in Figure 8. The $Cu2p_{1/2}$ and $Cu2p_{3/2}$ peaks appeared at 952 and 932 eV without significant shifts for all *Cu*, *LaCu*, and *NdCu*. Absence of significant shifts indicated that electronic states of Cu(II) ions (which might be sensitive to charge transfer observed by optical spectra) are kept regardless of not only introducing (presence) or absence of 4f ions but also difference of diamagnetic or paramagnetic 4f ions for these compounds. As mentioned above, the differences of $\chi_M T$ vs T plots indicated antiferromagnetic superexchange interactions for *NdCu* [18] and merely paramagneric behaviour for *Cu* and *LaCu*. Hence we could confirm that electronic (valence) states of Cu(II) ion were not different among *Cu*, *LaCu*, and *NdCu* regardless of magnetic superexchange interactions [19] or addition of 4f ions by means of XAS.

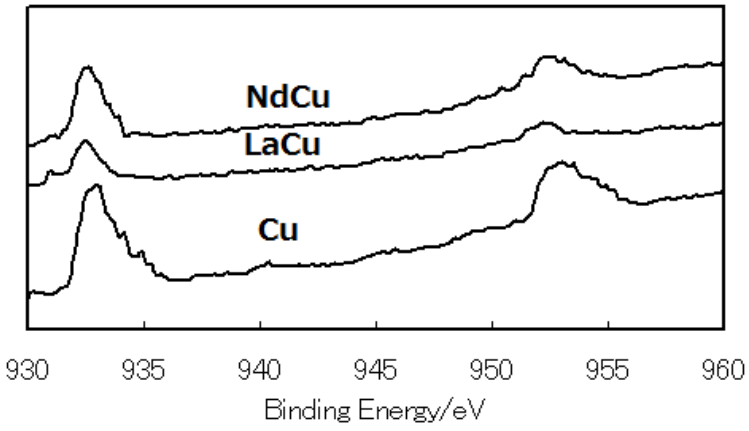

Figure 8. The XAS of $Cu2p_{1/2}$ and $Cu2p_{3/2}$ peaks for *Cu*, *LaCu*, and *NdCu*.

Diffuse Reflectance and Solid-State CD Spectra

Figures 9, 10, and 11 depict diffuse reflectance electronic spectra and the corresponding solid-state CD spectra for Ni(II) complexes (*Ni*, *LaNi*, and *NdNi*), Cu(II) complexes (*Cu*, *LaCu*, and *NdCu*), and Zn(II) complexes (*Zn*, *LaZn*, and *NdZn*), respectively. For *NdNi*, *NdCu*, and *NdZn*, sharp f-f transitions due to Nd(III) ions are observed as two peaks in 12000-14000 cm^{-1}, though the corresponding solid-state CD bands are not clear. In this way, we must find other chiroptical characteristics based on CD spectra as well as electronic spectra for systematic compounds.

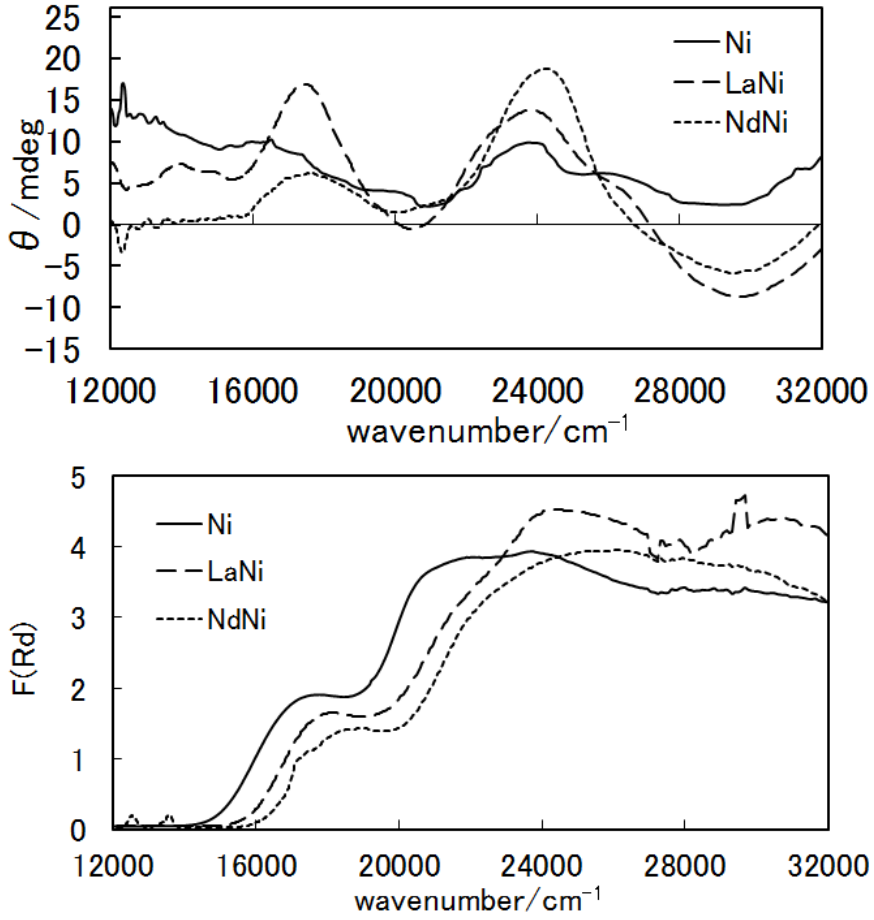

Figure 9. The diffuse reflectance electronic spectra and solid-state CD spectra for *Ni*, *LaNi*, and *NdNi*.

As shown in Figure 9, diffuse reflectance electronic spectra appeared obvious d-d bands at 17000 cm^{-1} for *Ni*, 18000 cm^{-1} for *LaNi*. Shoulders due to CT bands are observed at 21000 cm^{-1} for *Ni*, 22000 cm^{-1} for *LaNi*, and 22000 cm^{-1} for *NdNi*, 18000 cm^{-1}. The π–π* bands appeared at 24000 and 30000 cm^{-1} for *Ni*, 24000 and 30500 cm^{-1} for *LaNi*, and 24000 and 30500 cm^{-1} for *NdNi*. Introducing 4f ions resulted in high-wavenumber shift of d-d and CT bands and splitting broad and intense π–π* bands. The corresponding CD spectra appeared d-d bands at 17500 cm^{-1} (positive) for *LaNi* and 18000 cm^{-1} (positive) for *NdNi*. The CT bands

(*Ni*, around 16000 cm^{-1}) are observed at 24000 cm^{-1} (positive) for *LaNi*, and 24000 cm^{-1} (positive) for *NdNi*. The π–π* bands could be observed at 32000 cm^{-1} (negative) for *LaNi*, and 32000 cm^{-1} (negative) for *NdNi*. Introducing 4f ions resulted in enhancing CD peaks, which could not be observed clearly for *Ni* taking different electronic structures associated with magnetic dipole transitions.

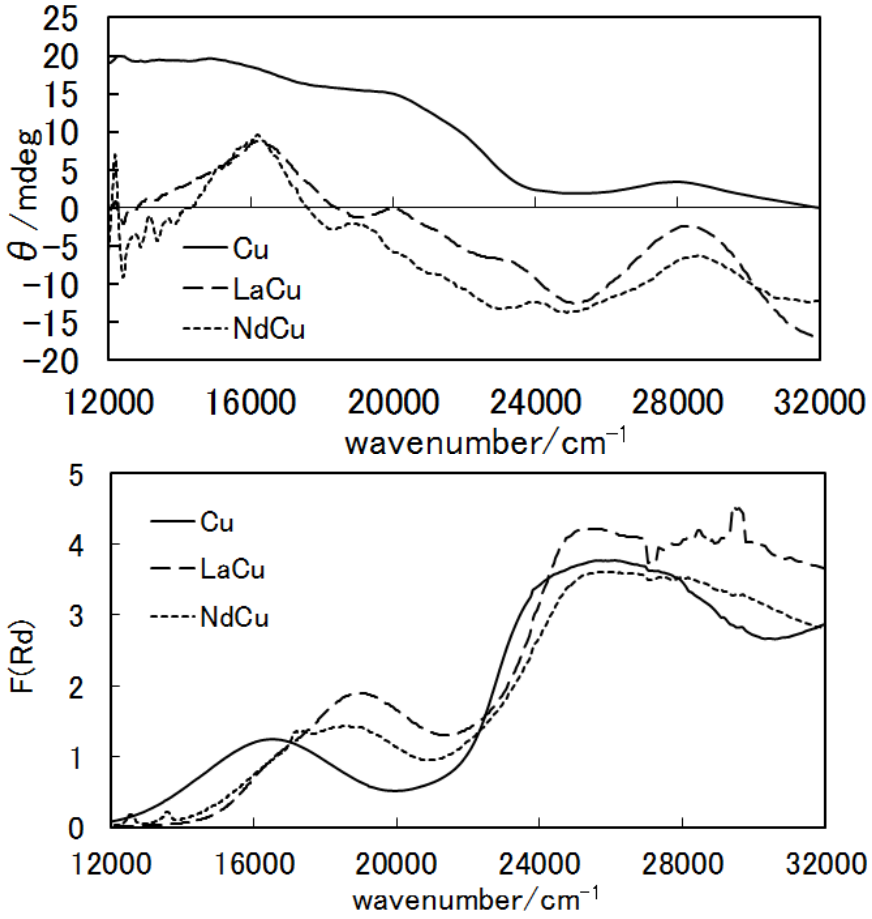

Figure 10. The diffuse reflectance electronic spectra and solid-state CD spectra for *Cu*, *LaCu*, and *NdCu*.

As shown in Figure 10, diffuse reflectance electronic spectra appeared obvious d-d bands at 16500 cm^{-1} for *Cu*, 19000 cm^{-1} for *LaCu* and 19000 cm^{-1} for *NdCu*. Shoulders due to CT bands are observed at 23500 cm^{-1} for *Cu*. The π–π* bands appeared at 25500 and more than 32000 cm^{-1} for *Cu*, 25000 cm^{-1} for *LaCu*, and 25000 cm^{-1} for *NdCu*. Introducing 4f ions resulted in slight high-wavenumber shift of CT bands and considerable high-wavenumber shift of d-d bands, which may be attributed to slight structural changes of coordination environment by solvents.

The corresponding CD spectra appeared d-d bands at 16000 cm^{-1} (positive) and 19000 cm^{-1} (negative) for *LaCu* and 16000 cm^{-1} (positive) and 19000 cm^{-1} (negative) for *NdCu*. The CT bands are observed at 22000 cm^{-1} (positive) for *Cu*, 24000 cm^{-1} (negative) for *LaCu*, and

24000 cm^{-1} (negative) for *NdCu*. The π–π* bands could be observed at 27500 cm^{-1} (positive) for *Cu*, 25500 cm^{-1} (negative) and 33000 cm^{-1} (negative) for *LaCu*, and 25500 cm^{-1} (negative) and 32000 cm^{-1} (negative) for *NdCu*. Introducing 4f ions resulted in decreasing of band widths of d-d region predominantly. Difference of the numbers of 4f electrons could be observed as slight shift in CT bands.

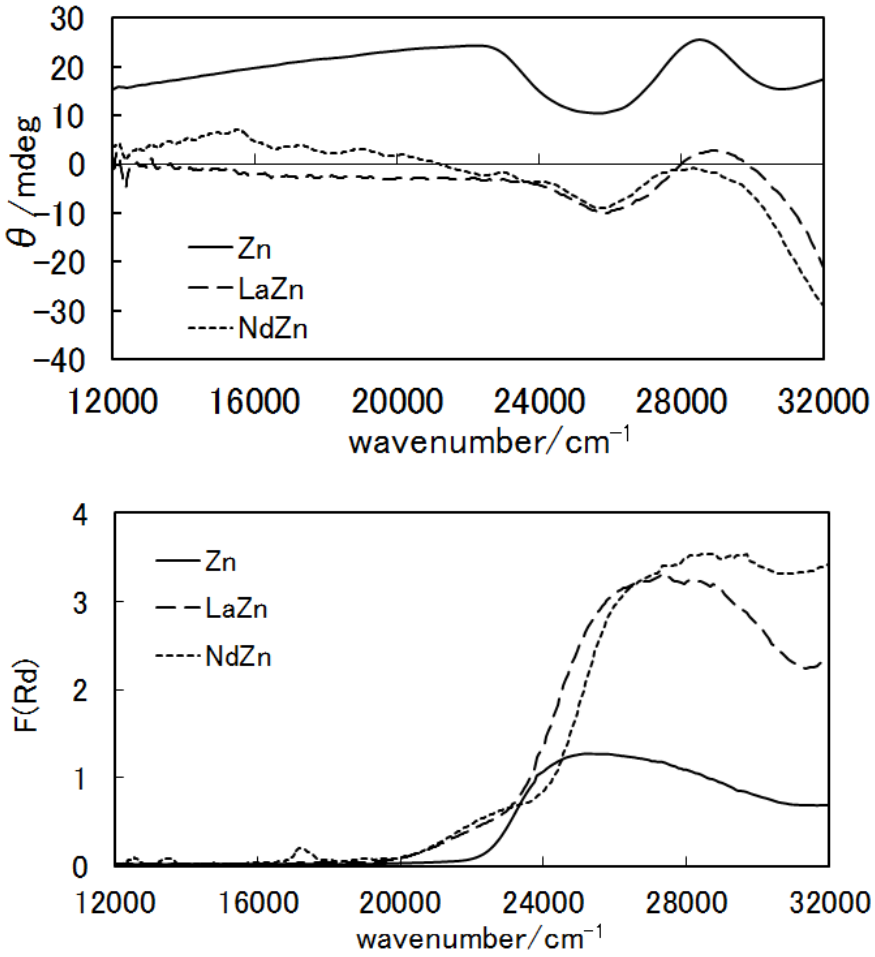

Figure 11. The diffuse reflectance electronic spectra and solid-state CD spectra for *Zn*, *LaZn*, and *NdZn*.

As shown in Figure 11, diffuse reflectance electronic spectra appeared CT bands as broad shoulders at 23500 cm^{-1} for *Zn*, 23000 cm^{-1} for *LaZn* and 23000 cm^{-1} for *NdCu*. The π–π* bands appeared at 25000 cm^{-1} for *Zn*, 28500 and 32000 cm^{-1} for *LaZn*, and 28500 and more than 32000 cm^{-1} for *NdZn*. Introducing 4f ions resulted in slight high-wavenumber shift of CT and π–π* bands, though Zn(II) complexes of $3d^{10}$ configuration do not exhibit d-d bands. The corresponding CD spectra appeared CT bands at 26000 cm^{-1} (positive) for *Zn*, 26000 cm^{-1} (negative) for *LaZn*, and 26000 cm^{-1} (negative) for *NdZn*. The π–π* bands could be observed at 28000 cm^{-1} (positive) and more than 32000 cm^{-1} (positive) for *Zn*, 28500 cm^{-1} (negative) and 32000 cm^{-1} (negative) for *LaZn*, and 28500 cm^{-1} (negative) and 32000 cm^{-1} (negative) for

NdZn. Introducing 4f ions resulted in low-wavenumber shift of CT and π–π* bands and decreasing of band widths. Assignment of CD bands have been considered as follows: A weak band around 16000 cm^{-1} was observed for *Ni* and *Cu*, while it was not observed and quite broad band in the range of 12000-23000 cm^{-1} for *Zn* (it may be so-called artifact peak of solid-state CD spectra). By comparing with 3d and 3d-4f complexes, d-d bands may be sensitive to structural changes by introducing 4f ions. Therefore, d-d, CT, and π–π* bands are observed in 12000-20000, 20000-28000, and more than 28000 cm^{-1}, respectively.

According to preliminary ZINDO (and also TD-DFT) calculations, simulated diffuse reflectance electronic spectrum of *Ni* appears weak d-d band around 400 nm, CT band around 320 nm, and strong π–π* bands around 270 and 220 nm. The corresponding simulated CD spectrum appears quite weak d-d band around 500 nm (negative) and 450 nm (positive), strong CT bands around 320 nm (positive) and 280 nm (positive), and quite strong π–π* bands around 220 nm (positive) and 200 nm (negative). Although mononuclear 3d complexes exhibit positive CD peaks of π–π* bands due to chiral ligands around 28500 cm^{-1}, binuclear 3d-4f complexes exhibit negative CD peaks in the corresponding region regardless of the identical chiral lingads of absolute structures. This is novel feature of solid-state chiroptical observation by forming 3d-4f units. The explanation can be given that introducing 4f ions (1) changes magnetic dipole moments, (2) changes molecular orbitals to show characteristic optical transitions. In order to examine (2), further study by for various $4f^n$ ions should be valid. Conventionally optical absorption (electronic) spectra (for single crystals) [20] and MCD [21] spectra have been employed for superexchange systems of asymmetric metal (not symmetric 3d-3d or 4f-4f) ions. At least we could observe characteristic chiroptical (CD) bands not for mononuclear 3d [22] or 4f [23] components but for binuclear 3d-4f systems.

CONCLUSION

In summary, we have prepared new chiral salen-type Schiff base binuclear 3d-4f and mononuclear 3d complexes to examine influence of 3d ions and introducing diamagnetic/paramagnetic 4f ions on structures, magnetic properties, and chiroptical properties. Only five crystal structures have been determined to reveal that all binuclear 3d-4f complexes forms dimmeric units connected by intermolecular hydrogen bonds. Since only Cu(II) and Nd(III) ions are paramagnetic, *Cu*, *LaCu*, *NdCu*, *NdNi*, and *NdZn* are paramagnetic. Concerning paramagnetic behaviour of Cu(II) ion, *Cu* and *CuLa* exhibit merely paramagnetism, while *NdCu* exhibits antiferromagnetic superexchange interactions. Based on solid-state (electronic and) CD spectra even at room temperature for this systematic system, we could find characteristic features of π–π* bands (besides f-f peaks of Nd(III)) reflecting influence of not only 3d ions but also none, diamagnetic, and paramagnetic 4f ions for the first time. As far as the present compounds after introducing 4f ions, (1) changes direction and magnitude of magnetic dipole moment and transition; (2) transition energies associated with molecular orbital may be ascribed to novel chiroptical observation.

Although CD spectroscopy is widely employed to determine absolute structures of chiral compounds, detailed information derived from optical bands are not fully used similar to electronic spectra. Additionally, since 3d-4f systems are difficult to assign CD bands by means of computational chemistry, even qualitative interpretation of CD bands must be useful

for investigation of electronic properties 3d-4f compounds. Further studies on f-f transition are in progress now, which will be interesting and important in view of solid-state inorganic chemistry.

SUPPLEMENTARY DATA

Crystallographic Data

Crystallographic information will be available (CCDC 846772 for *Ni*, 846773 for *LaNi*, 846774 for *NdNi*, 846770 for *LaCu*, and 846771 for *NdCu*) from the Cambridge Crystallographic Data Centre, 12 Union Road, Cambridge CB2 1EZ, UK (e-mail: deposit@ccdc.cam.ac.uk).

ACKNOWLEDGMENTS

This work with synchrotron radiation was carried out at KEK-PF BL-8B (2010G511) and BL-19B (2010G510). The author thanks Institute for Molecular Science and the Materials Design and Characterization Laboratory, Institute for Solid State Physics University of Tokyo for the SQUID facilities.

REFERENCES

[1] Stiuabm S. A.; Paraschiv, C.; Kiritsakas, N.; Lloret, F.; Munck, E.; Bominaar, E. L.; Andruh, M. *Inorg. Chem.* 2010, 49, 3387-3401.
[2] Wilson, D. C.; Liu, S.; Chen, X.; Meyers, E. A.; Bao, X.; Prosvirin, A. V.; Dunbar, K. R.; Hadad, C. M.; Shore, S. G. *Inorg. Chem.* 2009, 48, 5725-5735.
[3] Li, G.; Akitsu, T.; Sato, O.; Einaga, Y. *J. Am. Chem. Soc.* 125 (2003) 125, 12396-12397.
[4] Chen, W.-T.; Wang, M.-S.; Cai, L.-Z.; Xu, G., Akitsu, T.; Akita-Tanaka, M.; Guo, G.-C.; Huang, J.-S., *Cryst. Growth & Design* 6 (2006) 1738-1741.
[5] Chen, W.-T.; Guo, G.-C.; Wang, M.-S.; Xu, G.; Cai, L.-Z.; Akitsu, T.; Akita-Tanaka, M.; Matsushita, A.; Huang, J.-S. *Inorg. Chem.* 46 (2007) 2105-2114.
[6] Akitsu, T.; Einaga, Y. *Inorg. Chim. Acta* 2006, 359, 1421-1426.
[7] Akitsu, T.; Einaga, Y. *Polyhedron* 2006, 25, 2655-2662.
[8] Akitsu, T.; Einaga, Y. *Asian Chem. Lett.*2006, 10, 95-102.
[9] Akitsu, T.; Einaga, Y. *Asian Chem. Lett.*2006, 10, 113-120.
[10] Akitsu, T.; Einaga, Y. *Chem. Pap.*2007, 61, 194-198.
[11] Figuerola, A.; Diaz, C.; Ribas, J.; Tangoulis, V.; Granell, J.; Lloret F.; Manhia, J.; Maestro, M. *Inorg. Chem.* 2003, 42, 641-649 and references therein.
[12] Akitsu, T. *Asian. Chem. Lett.* 14, 2010, 53-62.
[13] Yoon, J. H.; Yoo, H. S.; Kim, H. C.; Yoon, S. W.; Suh, B. J.; Hong, C. S. *Inorg. Chem.* 2009, 48, 816-818.

[14] Felices, L. S.; Escudero-Adan, E. C.; Benet-Buchhoiz, J.; Kleij, A. W. *Inorg. Chem.* 2009, 48, 846-853.
[15] Sutter J.-P.; Dhers, S.; Rajamani, R.; Ramasesha, S.; Costes, J.-P.; Duhayon, C.; Vendier, L. *Inorg. Chem*. 2009, 48, 5820-5828.
[16] Chi, Y.-X.; Niu, S.-Y.; Wang, .-L.; Jin, J. *Eur. J. Inorg. Chem*. 2008, 2336-2343.
[17] Sheldrick, G. M. *Acta Crystallogr*. 2008, A64, 112-122.
[18] Boca, R.; Herchel, R. *Coord. Chem. Rev*. 2010, 254, 2973-3025.
[19] Sinn, E. *Coord. Chem. Rev*. 1970, 5, 313-347.
[20] McCarthy, P. J.; Gudel, H. U. *Coord. Chem. Rev*. 1988, 88, 69-131.
[21] Piligkos, S.; Slep, L. D.; Weyhermuller, T.; Chaudhuri, P.; Bill, E.; Neese, F. *Coord. Chem. Rev*. 2009, 253, 2352-2362.
[22] Peacock, R. D.; Stewart, B. *Coord. Chem. Rev*. 1982, 46, 129-157.
[23] Brittain, H. G. *Coord. Chem. Rev.* 1983, 48, 243-276.